On verification of numerical hydrodynamic model of powder-based laser metal deposition process

IOP Conf. Series: Journal of Physics: Conf. Series **1109** (2018) 012004 doi:10.1088/1742-6596/1109/1/012004

On verification of numerical hydrodynamic model of powder-based laser metal deposition process

M.D. Khomenko[1], F.Kh. Mirzade[1], S. Pityana[2]

[1] Institute on laser and information technologies, Branch of FSRC "Crystallography and photonics" RAS, 1, Svyatoozerskaya str., Shatura, Russia, 140700

[2] National Laser Centre, Council for Scientific and Industrial Research, South Africa

Email: hmd@laser.ru

Abstract. The developed hydrodynamic model of laser cladding (LC) considering catchment efficiency is verified with experimental data for steel powder LC in a wide range of process parameters. The comparison of the main calculated output parameters (depth of the penetration, track width and height) with experimental data is held. The experimental track profile is compared with the results of the calculations. It is shown that the model works well even for unhealthy high dilution parameter sets and could be used for processing window search.

1. Introduction

Laser cladding (LC) is a fairly widespread additive manufacturing technology, but some shortcomings, such as, for example, a narrow processing window, limit its further progress. Direct numerical simulation (DNS) of LC has established itself as an effective supplementary method for determining optimal parameters and investigating the process [1]. The main challenge of DNS is the model and real life situation correspondence, so the conduction of validation and verification is critical for its successful application. The more reliable DNS models can boost the quality, flexibility and automation of direct fabrication.

The validation of numerical models is often performed by comparing numerical results with analytical solutions. LC is a complex multifactor problem, and it is difficult to obtain an analytical solution for the whole system. In such cases, a comparison of individual phenomena with their analytical description is held [2]. However, the agreement of distinct phenomena does not guarantee the model to work for the process as a complex. Either there are no satisfactory analytical solutions for adequate process parameters or the interaction of related phenomena with each other has a greater influence than a separate phenomenon. Therefore, verification is carried out by comparing the output parameters of LC with the results of calculations. A comparison with experimental data is made for separate (for example, cladding width) [3] and for sets of output parameters [4]. However, this approach verifies the correct behavior of the model only for processing parameters used. The comparison of the set of output parameters with experimental data for a wide range of process parameters, gives opportunity to speak about fundamental nature of the results and applicability of the model for determining the processing window. The derivative output parameters (for example, waviness, roughness [5] or microstructure [6]) are also important for the development of direct production of parts.

The great difference between single output parameter and the experimental data indicates that the model does not take into account the important phenomenon that affects the process. The thermal model,

for example, which does not take into account hydrodynamic effects, cannot correctly estimate the track spreading along the substrate and underestimates the melt pool width [7]. There are situations when a good correspondence of the track integral characteristics does not lead to a coincidence of the track profile [4], which reveals the drawbacks of the model. The purpose of this paper is to verify the previously developed hydrodynamic LC model in a wide range of process parameters.

2. Physical model

The model is developed on the basis of the open CFD package OpenFoam. It includes heat and mass transfer in a multiphase system: gas - liquid melt pool - solid substrate. Numerous coupled phenomena take place in the melt pool, so special attention is paid for solving the self-consistent system of equations, where heat conduction, convection and the free surface motion are taken into account simultaneously. The hydrodynamic macromodel is described in detail in [8] and is not given here. The main driving force is surface thermocapillary force [4]. Its competition with capillary forces determines the shape of the clad track. These surface forces in a three-phase model are introduced as volumetric sources [9]. The phase change in the melt pool is modeled as a porous medium [10] which takes into account of the fluid flow drag at the solid boundary. To monitor the free metal-gas interface, a VOF-like method is used [11]. The free surface is supposed to move with a normal velocity q_{powder}, related to the powder feed:

$$\frac{\partial \alpha}{\partial t} + \nabla \cdot (u\alpha) = q_{powder} \left| \nabla \alpha \right| \quad (1)$$

Within this model, the powder was captured in the liquid melt pool:

$$q_{powder} = F_l(x, y, z) \frac{2\alpha_p \dot{m}}{\pi \rho R_{jet}^2} \exp(-\frac{2r(x, y)^2}{R_{jet}^2}) \quad (2)$$

where F_l is the flag of substrate state ($F_l = 1$ on a liquid substrate and $F_l = 0$ on a solid substrate), α_p is the catchment efficiency ratio, $\dot{m}$ is the powder feed rate, and R_{jet} is the powder jet radius on the substrate.

Table 1. Thermal parameters used for the simulation.

Property	Parameter, units	Value	Property	Parameter, units	Value
Heat conductivity of solid metal	W/(m*K)	44	Dynamic viscosity of metal	10^{-7} m^2/s	6.989 [12]
Heat conductivity of liquid metal	W/(m*K)	40	Dynamic viscosity of air	10^{-5} m^2/s	1.48
Heat conductivity of air	W/(m*K)	0.03	Surface tension	N/m	1.872 [12]
Density of metal	kg/m^3	7870	Surface tension gradient	mN/m*K	-0.49 [12]
Density of air	kg/m^3	1	Latent heat capacity	kJ/kg	247.1
Heat capacity of solid	J/(kg*K)	659	Catchment efficiency ratio	-	1
Heat capacity of liquid	J/(kg*K)	804	Absorption coefficient	-	0.45
Heat capacity of air	J/(kg*K)	1008	Beam radius	mm	2
Solidus temperature	K	1789	Jet radius	mm	1.5
Liquidus temperature	K	1819	Powder temperature	K	1000

3. Results and discussion

With the help of the developed model, parametric studies of single tracks of AISI 431 powder LC were made on a steel substrate. An experimental study was carried out, which is described in detail in [7]. The material parameters used in the calculations are presented in Table 1. At the initial time, the laser beam propagates in the positive direction of the x axis till the time when cladding parameters reach steady-state values.

Table 2. Process parameters and corresponding numerical and experimental data

Laser power, kW	Scanning speed, mm/s	Mass feed rate, g/min	Thermal model [7]			Experiment			Hydrodynamic model			
			width mm	depth µm	height, µm	width mm	depth µm	height, µm	width mm	depth µm	height, µm	Catchment
2.7	30	6		-		1975	604	233	1832	449	288	0.99
3.2						2084	298	233	1730	347	279	0.98
3.7						2024	217	250	1632	254	231	0.9
2.7	40	9	1445	327	245	2028	306	274	1762	350	287	0.94
3.2			1309	218	245	1657	209	274	1651	248	248	0.84
3.7			1036	136	245	1540	129	258	1426	172	154	0.58
2.7		22		-		1971	241	443	1783	252	529	0.95
3.2						1633	112	435	1612	148	531	0.83
3.7						1326	48	419	1402	80	415	0.56

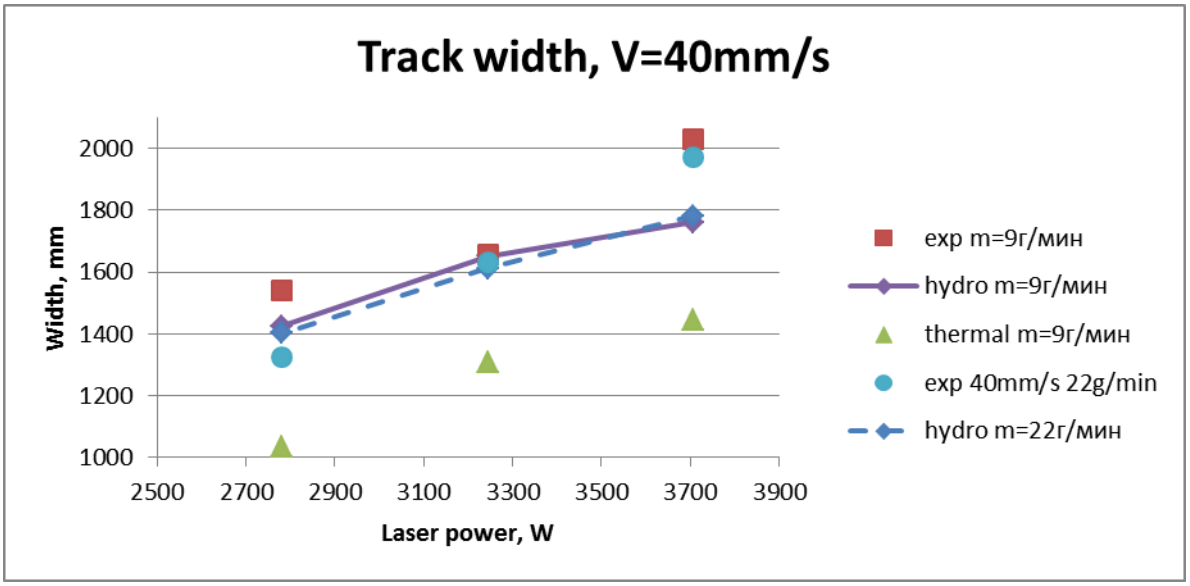

Figure 1. Track width dependence on laser power for scanning speed **V**=40mm/s

The numerical and experimental results for the studied process parameters are presented in Table 2. The calculations were carried out for a scanning speed of 30 mm/s and 40 mm / s. The presented results with **V**=40mm/s are treated as “low dilution” parameter sets. One “high dilution” parameter set was also investigated (**V**=30mm/s, m=6.76g/min) for the same laser power.

The results of the calculations are also compared with the numerical data for the thermal model [7]. Figures 1-3 show the comparison of calculated results with experimental data for “low dilution” parameter sets. It can be seen that the hydrodynamic model allows to more accurately determine the main parameters of LC. Figure 1 shows the dependence of the melt pool width on the laser power. The model gives reduced values at high and low power. The error is higher at high power, which is apparently

due to the nonlinearity of the coefficients that are not taken into account in the calculations. In general, the melt pool width is estimated better than in the thermal model; this is due to the fact that the spreading of the melt occurs precisely due to hydrodynamic forces.

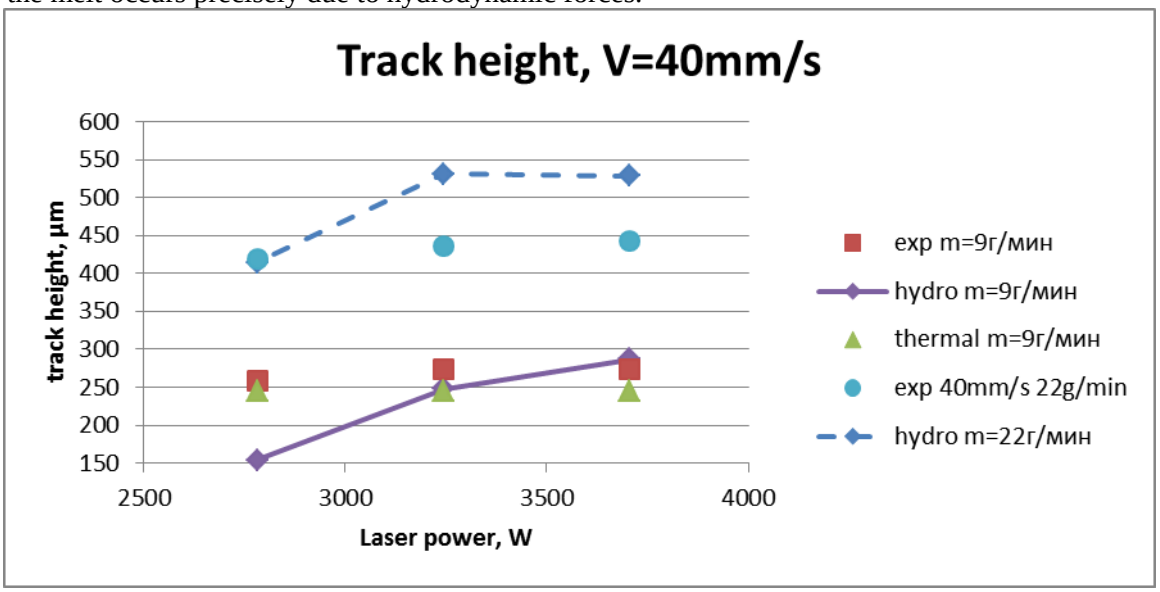

Figure 2. Track height dependence on laser power for scanning speed V=40mm/s

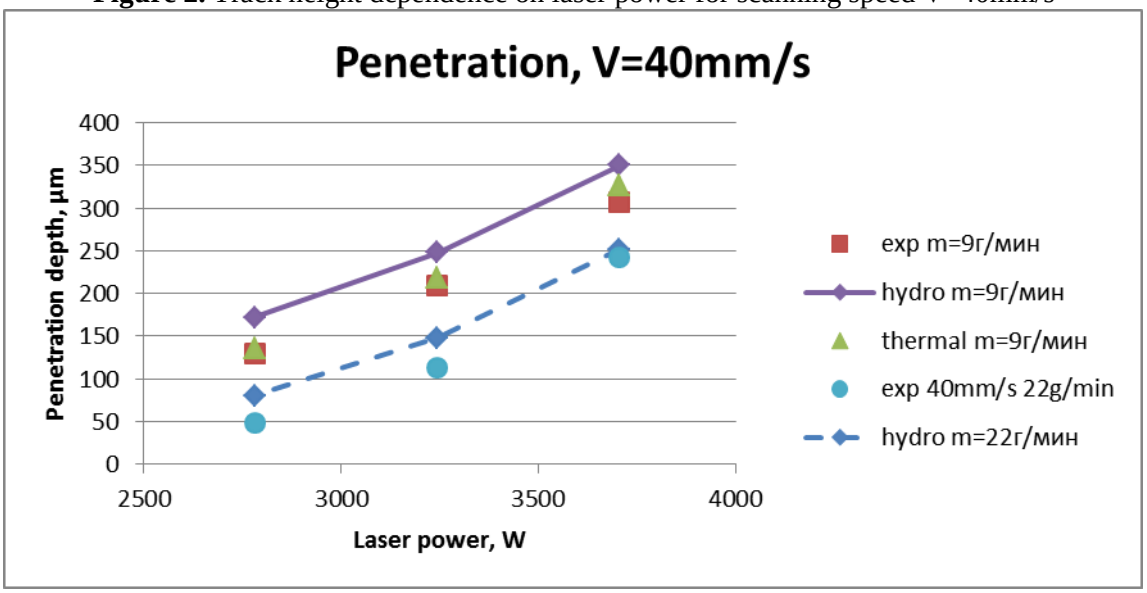

Figure 3. Penetration depth dependence on laser power for scanning speed **V**=40mm/s

Figure 2 shows the track height dependence on the laser power. At high and medium laser power, the height is well defined by the hydrodynamic model. With these two laser power values, the catchment efficiency ratio is maximal, and the track height does not change considerably with power increase. At low power, the calculations show a decrease in the width and lag of the melt pool from the front edge of the beam, which leads to a decrease in the degree of overlap with the powder jet. The developed model shows a decrease in the catchment efficiency (Table 2) and, as a consequence, a decrease in the deposition height at low laser power. This decrease is not so significant as in the experiment, that, apparently, is due to incorrect calculation of the reduction of the degree of the melt pool and powder jet intersection. A single catchment efficiency ratio is used in the model for the two powder feed rates. It is seen that in the case of large value, the model gives an overestimate of the cladding height, which is apparently due to the different value of this ratio for high and low powder feed rate in a real situation.

Figure 3 shows the dependence of the depth of penetration on the power of the laser radiation. The model gives somewhat exaggerated results for the investigated values of powder feed rate. The depth of penetration almost linearly increases with increasing laser power. Some nonlinearity is visible in the case of a large value of the mass feed rate.

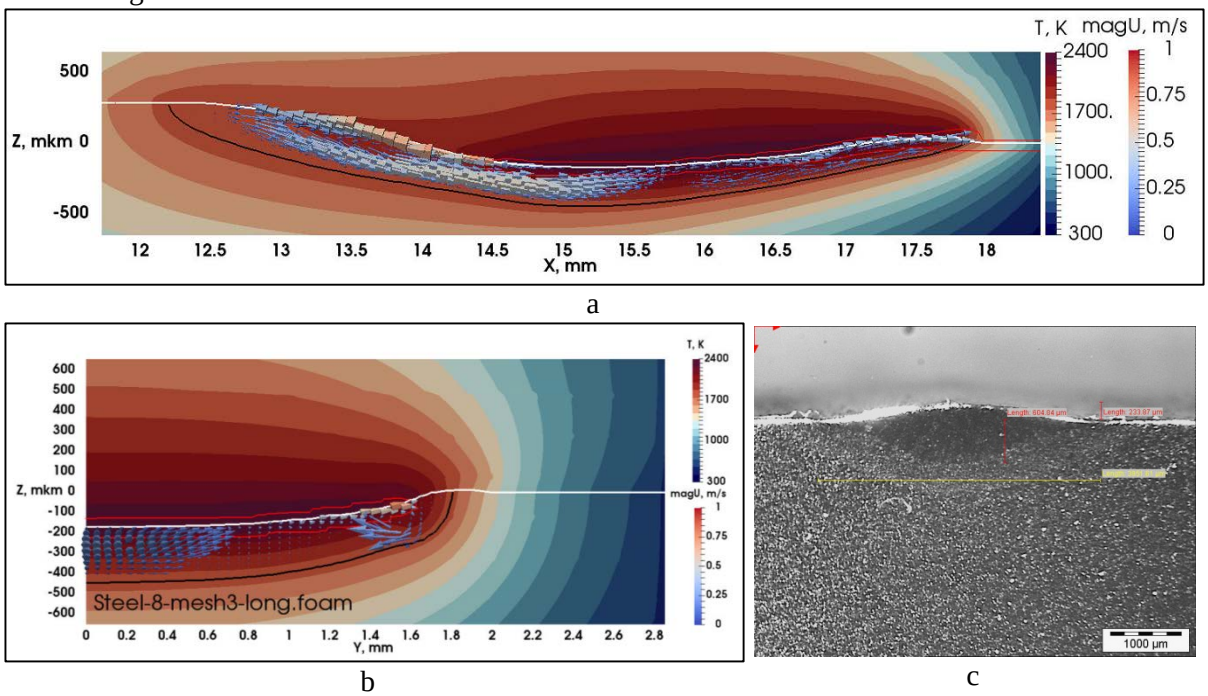

Figure 4. Numerical melt pool temperature cross-sections along (a) and across (b) the beam scanning direction. Experimental cladded track transversal cross-section (c). **V**=30mm/s, m=6.76g/min, P=3707W. Arrows show numerical fluid flow velocity.

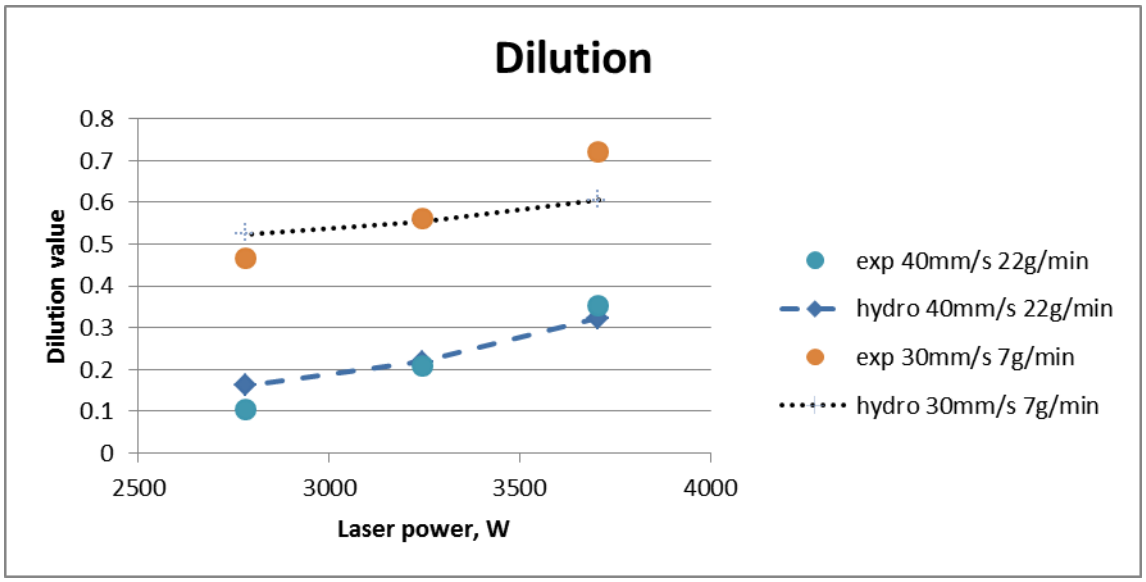

Figure 5. Dilution dependence on laser power for two parameter sets.

It is known that the main melt flow source is located directly behind the topHat beam [8]. Due to the position of the melt pool relative to the laser beam huge current may occur in appropriate direction. Figures 4 a, b show the melt pool cross-sections along and across the beam scanning direction. The black line indicates the melt pool boundary, the red contour is the 90% of laser power absorption, and

arrows indicate numerical fluid flow velocity magnitude. In our case melt pool is longer and narrower than laser beam (R_{beam}=2mm). The main current on the surface occurs against scanning speed. The free surface subsidence is essential at high laser power. Its increase is due to higher temperature gradient in that case. Such subsidence results in extremely high dilution and penetration values (Figure 3c). The melt pool is deformed by the fluid flow at high laser power and high penetration is seen in the track center. It might be supposed that penetration maximum would be at the track edge for the melt pool wider than laser beam and the main current on the surface would be in transverse direction.

Figure 5 shows dilution values for “low dilution” and “high dilution” processing parameters. Very good agreement of the hydrodynamic model is seen for “low dilution” set of parameters. The agreement is worse for “high dilution” set but the model shows the unhealthy dilution increase at high laser power so it could be used for finding the processing window borders.

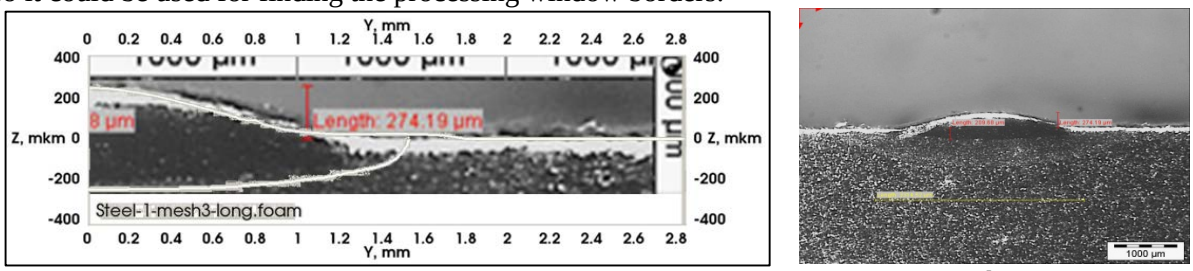

a b

Figure 6. Track profile comparison with numerical results shown by white lines (a). Optical microscope photograph (b) **V**=40mm/s, m=9g/min, P=3244W

Figure 6 shows comparison of track profile with numerical results. Excellent coincidence is obtained for presented processing parameters. The numerical results has slight concave form which is not seen in the in the track gained experimentally. Also the current across the scanning direction results in wide and low track edge which is not verified by the experiments. This might be due to wrong track-substrate contact angle received from the model and might be corrected using the measured contact angle [13].

4. Conclusion

A comparison is made between the macroscopic parameters of the clad track for the hydrodynamic LC model taking into account the powder catchment efficiency. In general, it was possible to obtain a good correspondence between the calculated and experimental data in a wide range of technological parameters. The error in determining the melt pool width was, on average, 6% for the “low dilution” parameters studied and 16% for the track height. Worst of all, the model determines the depth of penetration, here the error was 33%, nevertheless this can be considered a satisfactory agreement with the experiment. The simulated clad profiles agree well with the experiment.

In the further work, it is planned to compare track microstructure with the values obtained experimentally. Matching of the calculated parameters with experimental data makes it possible to refine the numerical model and understand the calculation parameters for real conditions. The verified model can be used to search for the processing window of the LC process. Direct numerical simulation is a convenient tool both for planning and optimizing the LC process itself, and for the feedback systems tuning.

Acknowledgements

This work was supported by the Federal Agency of Science Organizations (agreement № 007-ГЗ/Ч3363/26)

References

[1] Pinkerton A J 2015 Advances in the modeling of laser direct metal deposition *J. Laser Appl.* **27** S1
[2] Yamamoto T, Okano Y and Dost S 2016 *Int. J. Numer. Meth. Fluids* **83** (3), 223-44

[3] Zhang H O, Kong F R, Wang G L and Zeng L F 2006 *Journal of Applied Physics* **100,** 123522

[4] Qi H, Mazumder J and Ki H 2006 *Journal of Applied Physics* **100,** 024903

[5] Gharbi M, Peyre P, Gorny C, Carin M, Morville S, Le Masson P, Carron D and Fabbro R 2013 *Journal of Materials Processing Technology* **213**, 791– 800

[6] Acharya R, Sharon J A and Staroselsky A 2017 *Acta Materialia* **124**, 360-71

[7] Mirzade F Kh, Niziev V G, Panchenko V Y, Khomenko M D, Grishaev R V, Pityana S and Van Rooyen C 2013 *Physica B: Condensed Matter* **423**, 69–76

[8] Niziev V G, Mirzade F Kh and Khomenko M D 2018 *Quantum Electronics* **48** (8), 743 – 8

[9] Brackbill J U, Kothe D and Zemach C 1992 *Journal of Computational Physics* **100**, 335–54

[10] Voller V R, Prakash C 1987 *Int. J. Heat Mass Transfer* **30** (8), 1709-19

[11] Albadawi A, Donoghue D B, Robinson A J, Murray D B and Delauré Y M C 2013 *International Journal of Multiphase Flow* **53**, 11–28

[12] Gale W F, Totemeier T C 2004 *Smithell's Metals Reference Book* (London: Elsevier)

[13] Khomenko M D, Mirzade F Kh 2018 On the role of capillary and thermocapillary phenomena on microstructure at laser cladding *CEUR* (in press)